BIOCHEMISTRY
including biophysical chemistry & molecular biology

Article

pubs.acs.org/biochemistry

Membrane Interaction of the Factor VIIIa Discoidin Domains in Atomistic Detail

Jesper J. Madsen,[†,‡,⊥] Y. Zenmei Ohkubo,[§] Günther H. Peters,[‡] Johan H. Faber,[†] Emad Tajkhorshid,[*,§,∥] and Ole H. Olsen[*,†]

[†]Global Research, Novo Nordisk A/S, DK-2760 Måløv, Denmark

[‡]Department of Chemistry, Technical University of Denmark, DK-2800 Kgs. Lyngby, Denmark

[§]Beckman Institute for Advanced Science and Technology and [∥]Department of Biochemistry, College of Medicine, and Center for Biophysics and Computational Biology, University of Illinois at Urbana-Champaign, Urbana, Illinois 61801, United States

Supporting Information

ABSTRACT: A recently developed membrane-mimetic model was applied to study membrane interaction and binding of the two anchoring C2-like discoidin domains of human coagulation factor VIIIa (FVIIIa), the C1 and C2 domains. Both individual domains, FVIII C1 and FVIII C2, were observed to bind the phospholipid membrane by partial or full insertion of their extruding loops (the spikes). However, the two domains adopted different molecular orientations in their membrane-bound states; FVIII C2 roughly was positioned normal to the membrane plane, while FVIII C1 displayed a multitude of tilted orientations. The results indicate that FVIII C1 may be important in modulating the orientation of the FVIIIa molecule to optimize the interaction with FIXa, which is anchored to the membrane via its γ-carboxyglutamic acid-rich (Gla) domain. Additionally, a structural change was observed in FVIII C1 in the coiled main chain leading the first spike. A tight interaction with one lipid per domain, similar to what has been suggested for the homologous FVa C2, is characterized. Finally, we rationalize known FVIII antibody epitopes and the scarcity of documented hemophilic missense mutations related to improper membrane binding of FVIIIa, based on the prevalent nonspecificity of ionic interactions in the simulated membrane-bound states of FVIII C1 and FVIII C2.

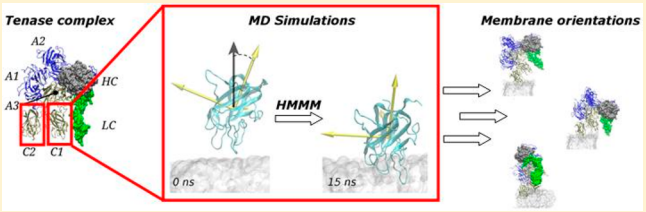

The biochemical processes governing blood clotting are classically represented by a "waterfall" or "cascade" model.[1,2] Two distinct pathways (intrinsic vs extrinsic) funnel into a common amplification phase where activated factor X (FXa) is generated, which, together with its cofactor FVa, is responsible for the burst of thrombin that subsequently leads to fibrin clot formation. The biomolecular components FVIII and FIX are circulating in the bloodstream as their inactive precursors, which upon activation assemble on a phospholipid surface into the highly potent FX-activating (FXase, also termed tenase) complex. Hemophilia A, the most common bleeding disorder by far,[3] is characterized by deficiency in FVIII activity observed either as low levels, dysfunction of the protein procofactor, or the presence of inhibitory antibodies.

A pivotal aspect of the coagulation cascade is the ability of restricting blood clotting to the injury site. The platform for this spatial localization is provided by the activated platelet membrane surfaces, which attract and stimulate activity by means of both membrane composition and the presence of elevated levels of certain cofactors to the coagulation enzymes. The tenase components FIXa and FVIIIa have the ability to selectively recognize this platform. Once the components are properly bound and the binary complex is formed, the catalytic efficiency of FIXa is upregulated by approximately five orders of magnitude.[4] Membrane binding modes of FVIIIa and FIXa, however, are quite different; FIXa is anchored to the membrane by its vitamin K-dependent γ-carboxyglutamic acid-rich (Gla) domain, while the membrane-targeting modules of FVIIIa are the two C2-like discoidin domains, C1 and C2, which recognize phosphatidylserine (PS)-containing platelet or endothelial cell membranes in a Ca^{2+}-independent manner.[5] While either domain (FVIII C1 or FVIII C2) by itself appears to be able to recruit the entire cofactor molecule to phospholipid membranes,[6−10] optimal biological activity most certainly requires both.

The active cofactor molecule, FVIIIa, consists of three polypeptide chains forming five major domains (A1, A2, and light chain A3−C1−C2) with a total of more than 1200 amino acid residues. The structural topology of the C1 and C2 domains is that of lectin and commonly known as a jellyroll β-barrel (Figure 1A); eight antiparallel β-strands are arranged in two major β-sheets, wrapped to form the barrel and then flattened to a sandwichlike shape.[11] Connecting the β-strands at the bottom of the barrel are four hairpin loops also called the spikes [S1−S4 (Figure 1A)] or fatty feet,[12] the latter

Received: April 17, 2015
Revised: September 2, 2015
Published: September 8, 2015

DOI: 10.1021/acs.biochem.5b00417
Biochemistry 2015, 54, 6123−6131

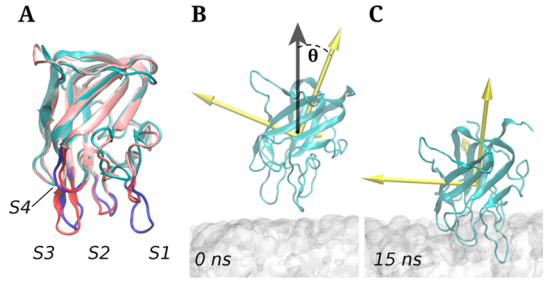

Figure 1. (A) Structural alignment of FVIII C1 (pink) and FVIII C2 (cyan) based on Protein Data Bank entry 3cdz.[22] Spikes (S1−S4) are colored red for FVIII C1 and blue for FVIII C2. (B) Representative domain orientation and position of the C2-like domain with respect to the surface of the membrane patch that was used in all the simulations as the starting configuration at 0 ns. Depicted are FVIII C2 (in cartoon representation) and the HMMM patch (translucent gray). The yellow vectors show the principal axes of inertia of the FVIII C2 domain. The domain tilt angle, θ, is defined as the angle between the third principal axis of inertia and the membrane normal, z (gray vector). (C) Representative membrane-bound state of FVIII C2 with inserted spikes (snapshot taken at 15 ns from trajectory 2).

designation being due to the presence of multiple solvent-exposed hydrophobic residues. These spikes are of particular importance for platelet membrane-aided functionalities because S1−S4 are hypothesized to be inserted into the hydrophobic core of the phospholipid membrane.[7,13] For this reason, much attention has been dedicated in the literature (e.g., by alanine mutagenesis,[14] motif mutagenesis,[15] and loop swaps[12]) to elucidate how the affinity and specificity of the FVIIIa molecule (and FVIII C2 on its own) toward phospholipid membranes are controlled by the residues in these spikes. The primary membrane-anchoring domain of FVIIIa is conventionally thought to be the C2 domain.[16] Recently, however, several studies have emphasized the important role of the C1 domain in the membrane-mediated cofactor function of FVIIIa.[6,8,15,17−21]

Previous studies of the molecular orientation of FVIIIa suggest a crystal structure-like domain configuration with a membrane-bound configuration in which the molecule is close to perpendicular to the membrane plane (or slightly tilted) with both FVIII C1 and FVIII C2 peripherally inserted into the membrane.[22−24] A fundamentally different interaction, requiring large scale domain rearrangements to accommodate a binding mode where solely FVIII C2 interacts with the membrane and is deeply inserted, has been suggested on the basis of cryo-electron microscopy experiments in conjugation with a membrane model consisting of lipids assembled on nanotubes.[25−28] In addition, the concurrent domain conformational span between C1 and C2 has been reported for the homologous coagulation factor Va in a study utilizing atomic force microscopy.[29]

The membrane interaction of FVIII C2-like domains has very recently been explored using molecular simulations at the coarse-grained level of theory.[30] While coarse-graining can be appropriate for comparing membrane binding times between domains and mutants, unfortunately atomistic details possibly governing specific interactions with the membrane are not readily discernible. Therefore, we have conducted all-atom simulations to give a detailed characterization of the individual discoidin domains from human coagulation FVIIIa in the membrane-bound state with respect to lipid specificity, molecular orientation, and flexibility. These are properties of fundamental importance for the cofactor activity of FVIIIa in the intrinsic tenase complex. The all-atom classical molecular dynamics (MD) simulation technique provides sufficiently high spatial and temporal resolutions to generate detailed information about the atomic level of the membrane binding and lipid interaction of the FVIIIa C2-like domains. To expedite the dynamics of membrane lipids and therefore accelerate the membrane binding of the C2-like domains, the use of the highly mobile membrane-mimetic (HMMM) model[31] is adopted. This allows multiple occurrences of membrane binding in relatively short, independent trajectories and provides a description of the protein−membrane interaction in good agreement with that of conventional full-tail lipid membrane models.[32] Hence, an improved statistical representation of the dynamics becomes feasible.

This article is structured as follows. The protein−lipid interaction of each of the two membrane-anchoring discoidin domains from human FVIIIa (FVIII C2 and FVIII C1) is characterized, and a PS-binding motif is described. The achieved membrane-bound states are discussed in relation to hemophilic disease mutations, antibody-binding epitopes, and a putative tenase complex model.

MATERIALS AND METHODS

Model Building and Initial Setup. The starting structures of FVIII C1 and FVIII C2 domains were taken from the crystallized B-domain-less human FVIII with Protein Data Bank (PDB) entry 3cdz[22] (residues 2021−2172 for FVIII C1 and residues 2173−2332 for FVIII C2). It can be safely assumed that there is little or no structural distinction between these domains in FVIII and FVIIIa, in the context of the full-length (pro)cofactor and cut out on their own. pK_a calculations were performed using PROPKA[33] to assign protonation states to titratable side chains consistent with pH 7; no deviation from standard titration states was necessary.

To assemble the HMMM membrane,[31] short-tailed (st) lipid molecules truncated at the C_5 atom containing a PS headgroup [i.e., divalerylphosphatidylserine (DVPS); see ref 31 for the details] were packed to sandwich a layer of 1,1-dichloroethane (DCLE) solvent molecules with the lipid headgroups facing the water phase and acyl chains against the DCLE organic phase using Packmol.[34] The technical advantage of using pure PS membrane patches is that issues relating to mixing of lipids of different type are nonexistent and the efficiency of locating PS-interacting residues of the protein is enhanced. Most likely, the PS concentration will have a negligible effect on the membrane-bound configurations of the C2-like domains, as long as it is sufficiently high.

The individual FVIII C1 and FVIII C2 domains (Figure 1A) were then manually placed above the membrane such that the β-barrel central axis (the third principal axis of inertia) was oriented approximately parallel to the membrane normal [$\theta \sim 0$ (Figure 1B)] with the hydrophobic membrane-anchoring spikes facing the membrane (Figure 1B). The spikes are defined as follows. S1 consists of residues 2043−2046 for FVIII C1 and 2196−2203 for FVIII C2, S2 residues 2056−2059 for FVIII C1 and 2213−2217 for FVIII C2, S3 residues 2089−2096 for FVIII C1 and 2248−2255 for FVIII C2, and S4 residues 2156−2159 for FVIII C1 and 2313−2316 for FVIII C2. The resulting systems (denoted C2/HMMM and C1/HMMM) that contained an HMMM patch and a C2-like domain were solvated by water molecules and neutralized with sodium (Na^+) ions using the SOLVATE and AUTOIONIZE

DOI: 10.1021/acs.biochem.5b00417
Biochemistry 2015, 54, 6123−6131

Table 1. Overview and Component Counts of the Simulated Systems

system	lipid type	area per lipid (Å^2)[a]	no. of trajectories	spontaneous binding observed	simulation time per trajectory (ns)	no. of water molecules	no. of atoms
C1/HMMM	PS	88.5	5	all except 1	50−55	∼7800	∼37000
C2/HMMM	PS	85.0	5	all	∼37	∼7700	∼37000
C2/Soln	–	–	1	–	50	∼4600	∼16400

[a]Before the insertion of the protein.

plug-ins of VMD.[35] Water molecules placed by SOLVATE within the DCLE organic solvent phase of the membrane (because of the presence of initially large gaps) were removed. A reference system was prepared in a similar fashion and contained only FVIII C2 in bulk water (C2/Soln) at a physiological NaCl concentration of 150 mM. The details of the individual systems simulated are listed in Table 1.

Simulation Details. The prepared systems (C2/HMMM and C1/HMMM) were initially energy-minimized by applying the conjugated gradient method for 5000 steps. Then the systems were subjected to a short (100 ps) simulation in the *NPT* ensemble with a constant aspect ratio of the membrane plane (x/y) to resolve imperfect packing of DCLE molecules and hence equilibrate the membrane thickness. During this phase, the area per lipid in the systems was free to change, and resulting values ranged from 85.0 to 88.5 Å^2 (prior to protein insertion). While this is somewhat larger than the values for pure lipid bilayers,[36,37] it is designed to take into account the approximate area that would be occupied by insertion of the protein domains. Once the membrane thickness was stable, a mild harmonic constraint with a small force constant of 0.01 kcal mol^{-1} Å^{-2} along the z-axis was applied on the C_2 atoms of all st-lipids to restrain them around the average height of all C_2 atoms in their respective membrane leaflet. This was done to gently reduce vertical diffusion (along the z-axis) of the st-lipids and to eliminate potential net translation of the system along the z-axis, as well as to discourage lipid inversion. Using the resulting system as an initial structure, the production MD simulations were performed five times independently for each system in the *NPnAT* ensemble with the target pressure and temperature of 1 atm and 310 K, respectively, controlled by the Nosé−Hoover Langevin piston barostat[38,39] and the Langevin thermostat (damping coefficient of 5 ps^{-1}),[40] respectively. The solution system (C2/Soln) was prepared in the same way, except no treatments for the absent lipids. Throughout, pressure coupling was applied along the membrane normal, n (piston damping coefficient of 5 ps^{-1}, piston period of 100 fs, and piston decay of 50 fs).

Long-range electrostatic forces were calculated using the particle mesh Ewald (PME) method[41,42] with a grid spacing of approximately 1 Å and a fourth-order spline for interpolation. Electrostatic forces were updated every 4 fs. van der Waals interactions were cut off at 12 Å in combination with a switching function beginning at 10 Å. Periodic boundary conditions were applied in the x-, y-, and z-directions. All MD simulations were performed using NAMD 2.9[43] with the CHARMM27 force field/CMAP correction[44,45] for proteins, CHARMM36[46] for lipid topology, and the TIP3P model for water.[47] An integration time step of 2.0 fs was used for the velocity Verlet algorithm with SHAKE.[48] All analyses and visualization of molecular structures and trajectories were conducted using VMD 1.9.1;[35] calculation of van der Waals and electrostatic interaction energies between the protein and the membrane was done using the NAMDENERGY plug-in of VMD without PME. Plots were prepared using Grace (xmgrace, http://plasma-gate.weizmann.ac.il/Grace).

Calculation of Order Parameters for Backbone (C_i−N_i) Vectors. The backbone C−N vector was defined for each individual amino acid residue as the normalized vector pointing from the backbone carbonyl carbon atom to the backbone amide nitrogen atom. The protein was aligned over the trajectory by a root-mean-square deviation-based structural alignment on all heavy atoms. Following this, nematic order parameters were calculated as described by Cecchini et al.[49]

$$S_i^2 = \left\langle \frac{3}{2}(\hat{\mathbf{z}}_i \cdot \hat{\mathbf{d}}_i)^2 - \frac{1}{2} \right\rangle$$

where S_i^2 is the order parameter for the ith residue, $\hat{\mathbf{d}}_i$ (the director) is a unit vector describing the trajectory-averaged vector from C_i to N_i in residue i of the aligned trajectory, and $\hat{\mathbf{z}}_i$ is the instantaneous atomic $C_i - N_i$ unit vector for residue i. The brackets denote averaging over the trajectory. The frame rate for the analysis was 10 frames/ns. The order parameters assume values from 0 to 1, and they are a measure of how much the atomic backbone vectors fluctuate around their respective trajectory-averaged directions, indicating the flexibility of the backbone at that given position in the structure. The procedure described above was performed as described in the next paragraph to obtain the trajectory-averaged order parameter values.

Trajectory-Averaged Analyses for the Membrane-Bound State. The domain tilt angles of FVIII C1 and FVIII C2, membrane-contacting frequencies for each amino acid residue, and backbone order parameters were calculated for the membrane-bound state and averaged. Not the whole trajectories were used measuring these properties; the trajectories at the time when the domain is associated with the membrane based on a 5 Å proximity criterion were used. This amounted to discarding the initial ∼1−2 ns from the C2/HMMM trajectories and ∼2−4 ns from the C1/HMMM trajectories, because membrane binding was realized very quickly; the remaining data were then pooled and analyzed.

Construction of a Putative Model of the FVIIIa:FIXa Tenase Complex. A putative model of the FVIIIa:FIXa tenase complex was constructed on the basis of the recently published X-ray crystallographic structure of the FVa:FXa prothrombinase complex from the venom of the eastern brown snake.[50] The light chain of FIXa in the constructed tenase complex was modeled in a FVIIa-like extended conformation,[51] instead of an arched conformation adopted by procine FIXa with a partially disordered Gla domain (L chain of PDB entry 1pfx[52]). Homologous molecules (FVa vs FVIIIa, and FIXa vs FXa) were aligned, and the missing loops were constructed with the molecular modeling package Quanta (Molecular Simulations Inc., San Diego, CA). The atomic coordinates of the model are available upon request from the authors (J.J.M. or O.H.O.) and can also be found in a short version (α-carbons only) in the Supporting Information.

DOI: 10.1021/acs.biochem.5b00417
Biochemistry 2015, 54, 6123−6131

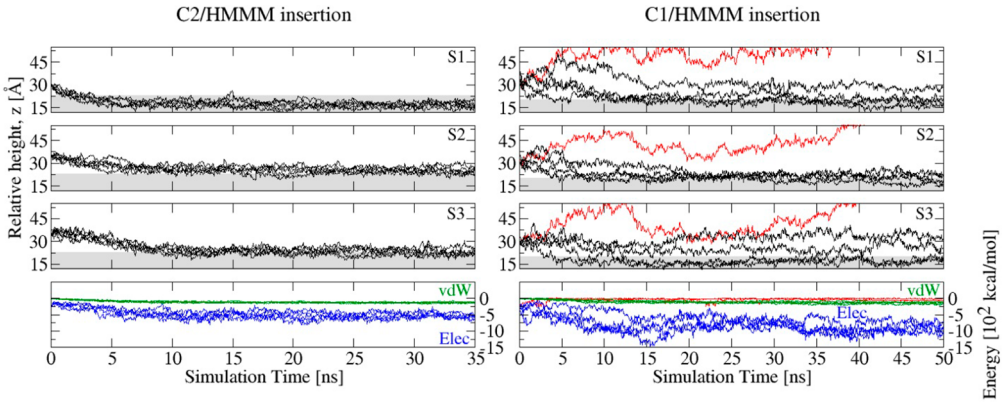

Figure 2. Insertion depth of S1−S3 of FVIII C2 and interaction energy with the HMMM as functions of the simulation time for the five trajectories, 1−5 (left panel). Each spike depth is represented by a single α-carbon atom, namely, G2044 for S1, S2058 for S2, and F2093 for S3. Insertion depth of S1−S3 of FVIII C1 and interaction energy with the HMMM as functions of the simulation time for the four binding trajectories, 2−5 (black), and for the unproductive (nonbinding) trajectory, 1 (red) (right panel). Each spike depth is represented by a single α-carbon atom belonging to a representative residue, namely, M2199 for S1, R2215 for S2, and L2252 for S3. In both panels, the gray-shaded area represents the membrane region below the average plane of the phosphate P atoms of st-lipids. The membrane is centered at z = 0. Calculated nonbonded interaction energies (bottom panels) are broken into van der Waals (vdW, green except for the unproductive simulation, which is colored red) and electrostatic (Elec, blue) components.

RESULTS AND DISCUSSION

Membrane binding simulations started with the anchoring domains initially placed over the membrane without any contacts. The positively charged FVIII C1 and FVIII C2 domains are attracted to the negatively charged phospholipid membrane because of favorable electrostatic interactions, shown by the calculated nonbonded interaction energies between the domain and the membrane (Figure 2, bottom, and Figure S1 of the Supporting Information). The difference in magnitude of the electrostatic interaction energy between FVIII C1 versus FVIII C2 and the membrane is rationalized by the fact that the former carries a larger net positive charge. As we describe in the following, the five parallel FVIII C2 trajectories converged into a stable membrane-bound state with comparable spike insertion depths and domain tilt angles (Figure 1C). The level of sequence identity shared by FVIII C1 and FVIII C2 is 40%, and structural alignment of the two shows a sub-angstrom root-mean-square deviation of 0.90 Å based on the crystal structure.[22] The amino acid residues directly involved in membrane binding and their specific sequence of interaction varied depending on the orientation of the studied FVIIIa domain upon membrane contact.

In the membrane-bound state of FVIII C2, a snug PS interaction via either R2220 or R2320 (Figure 3) was achieved. This configuration was not observed in any of the four membrane binding trajectories of FVIII C1 (one trajectory did not result in spontaneous binding and was discarded from further analysis), which instead displayed a broad range of domain tilt angles and significant structural modulations. Furthermore, the distinctive tight interaction of PS with the residue corresponding to R2320 in FVIII C1, R2163, was only observed in one trajectory. For both FVIII C1 and FVIII C2, the observed tightly bound lipid is further stabilized by polar interactions of the amino and phosphate groups with residues of the protein, but these depended on the lipid orientation at the PS specificity pocket.[13] These findings show that either domain can achieve a direct protein−lipid interaction where PS binds compactly. However, the observed propensities are surprising, considering experimental reports that show FVIII C2 binding to vesicles is not PS-specific.[53]

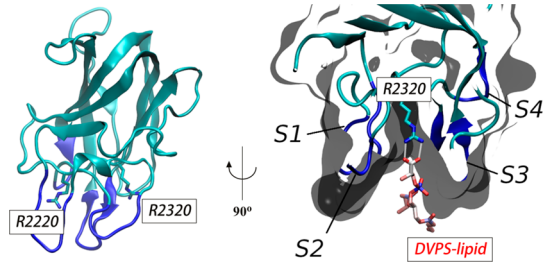

Figure 3. Positions of R2220 and R2320 in FVIII C2 with spikes (S1−S4) colored blue (left panel). Ninety degree-rotated (toward the right from the left panel) cross section of FVIII C2 (cyan wire presentation and black half-transparent surface; spikes colored blue) with a bound PS headgroup interacting with R2320 of the distinctive soft "funnel" PS pocket (right panel). A snapshot was taken from trajectory 5 at 21 ns.

FVIII C2 Adopts a Perpendicular Membrane-Bound Configuration and Achieves a Direct PS Interaction. The converged molecular orientation is characterized by the domain tilt angle (Figure 1B), which exhibited only small angles with respect to the membrane normal [20−40° (Figure 4, top)] and hence is consistent with the previously proposed perpendicular (or slightly tilted) mode of interaction[23] and also the respective entry in the OPM (Orientation of Proteins in Membranes) database[54] for FVIII (PDB entry 2r7e[55]). Regions of FVIII C2 in contact with the membrane were largely confined to the spikes (Figure 5, top). No significant structural modulations are observed for FVIII C2 upon membrane binding as indicated by the calculated backbone order parameters both for the membrane-bound simulations, C2/HMMM (Figure 5, top), and for FVIII C2 in bulk water, C2/Soln (Figure S2), albeit a mild overall stabilization can be detected for the membrane-bound form consistent with the conclusions of a recently published study of FVIII C2 by hydrogen−deuterium exchange mass spectrometry.[9]

The extruding hydrophobic spikes (Figure 1A) are inserted peripherally into the membrane as the relative height of the domain tends to decrease over time until convergence is achieved (Figure 2, left). The membrane-contacting surface is

DOI: 10.1021/acs.biochem.5b00417
Biochemistry 2015, 54, 6123−6131

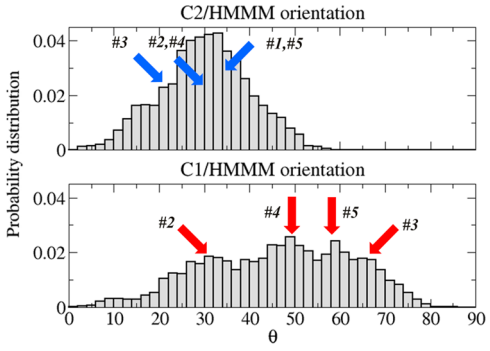

Figure 4. Distribution of the domain tilt angle, θ, of FVIII C2 (top) and FVIII C1 (bottom) for productive membrane binding trajectories (1–5 for FVIII C2 and 2–5 for FVIII C1). Domain tilt angles corresponding to the final configurations in individual trajectories (#1–5) are indicated by arrows.

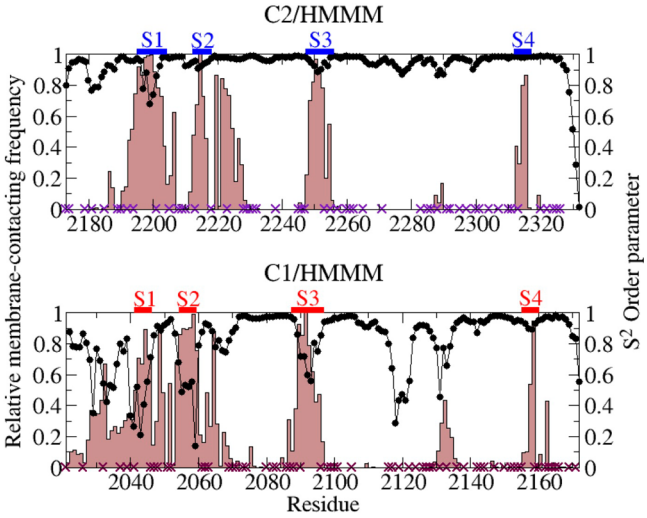

Figure 5. Backbone ($C_i - N_i$ vector) S^2 order parameters (●) and membrane contact frequencies (brown shaded bars) for FVIII C2 (top) and FVIII C1 (bottom) in their membrane-bound states. The positions of the spikes (S1–S4) are indicated above the panel (blue bars for FVIII C2 and red bars for FVIII C1). Hemophilic missense mutations are marked with crosses on the baselines.

confined to approximately one-third of the whole domain that mostly includes S1–S4 (Figure 1C). The basic residues of this region in FVIII C2 interact with the acidic PS lipids (either PO_4^- or COO^- functional group) in a mainly transient and nonspecific way with two exceptions, R2220 and R2320. It is the unique combination of a soft funnel-like geometry of the loops in the membrane-interacting part of the domain and a centrally positioned arginine (either R2320 or R2220 depending on the domain tilt angle) that interacts selectively with the carboxylic acid group of the lipid that defines the direct interaction with PS (Figure 3). This binding motif is further stabilized by polar interactions of the phosphate group of the lipid with surrounding amino acid residues of the protein.

It is interesting to note that while direct FVIII C2–PS interactions do occur, occasionally, via both R2320 and R2220, these residues seem to be mutually exclusive; in domain orientations that allow R2220 to be selectively engaged with the COO^- group of a PS lipid, R2320 cannot, and vice versa. Furthermore, the direct protein–PS interactions are observed less frequently than for FVa C2 studied previously.[56] In the study presented here, for FVIII C2, the direct lipid interactions of R2220 are found in two of the five trajectories (3 and 4), where they exist in ~80% of the simulation time in which the domain is membrane-bound. The R2320 interaction is found in two other C2/HMMM trajectories, 5 and 3, but only ~33 and ~10% of the membrane-bound simulation time, respectively.

A direct comparison with FVa C2 is complicated by subtle yet important differences in amino acid sequences and, in particular, by the fact that FVa C2 carries a net positive charge higher than that of FVIII C2, as conferred by a surplus of basic K and R residues over acidic D and E residues (+12 e for FV C2 and +6 e for FVIII C2). These differences have a direct impact on membrane affinity and association kinetics.[57] While binding free energies can, in principle, be calculated from a sufficiently long equilibrium simulation in which many binding/unbinding events occur, spontaneous membrane unbinding events have not been observed in this study nor in other reported work to the best of our knowledge.

FVIII C1 Exhibits Structural Flexibility and Has Multimodal Orientations in the Membrane-Bound State. While the profile of lipid interaction of FVIII C2 resembles that of FVa C2,[56] FVIII C1 is markedly different in two ways. First, while the trajectories again converge individually (Figure 2, right), a well-defined unimodal binding orientation is not achieved for FVIII C1 (Figure 4, bottom). Second, FVIII C1 in its membrane-bound form is characterized by shape modulations and disorder in the coiled main chain leading to spike 1 (Figure 5, bottom). There are two major contributions to the retardation of the binding motif that allow the FVIII C1 domain to adopt a variety of moderately to highly tilted molecular orientations in its membrane-bound form: (1) the loss of local structural integrity (Figure S3) and (2) the fact that spike 1 in FVIII C1 is four residues shorter than in FVIII C2, making it extrude significantly less (Figure 1A). The domain tilt angle is in general larger (relative to the membrane normal) for FVIII C1 than for FVIII C2; the averages of the angles for four individual C1/HMMM trajectories range between 30° and 65° (Figure 4, bottom).

The observed structural changes in FVIII C1 are facilitated by the breaking of the main chain H-bonds between Q2036 and K2072, which in the X-ray crystallographic structure clamp from the surrounding loop region to the body of the domain (Figure S3). Upon release, the main chain of the region centered around residue 2030 adheres to the membrane bilayer (Figure 5, bottom) and interacts favorably with it, but in a nonspecific manner. Such a structural mechanism or conformational change could explain, in part, why a complex multiphase binding mechanism is observed for FVIII.[58] The general trend of the calculated backbone order parameters clearly shows that FVIII C1 is more flexible than FVIII C2 (Figure 5), in particular in those regions that are in contact with the membrane (including the spikes, and the loop region leading to spike 1). Surprisingly, the C1 domain also exhibits increased flexibility in a loop, which is never observed to interact with the membrane (residues 2115–2123). The fact that FVIII C1 is relatively disordered (for such a β-rich domain) could further be involved in causing the scarcity of FVIII C1 domain structures available in the PDB.[59] There is supporting experimental evidence that those protein segments of FVIII C1 involved in the structural changes described above are indeed very flexible, as reflected in their high crystallographic temperature factors (PDB entries 3cdz[22] and 4bdv[60]).

DOI: 10.1021/acs.biochem.5b00417
Biochemistry 2015, 54, 6123–6131

A search for direct interactions between PS lipids and FVIII C1 (Figure S4, left) reveals that around the key positions in FVIII C1, R2163 [the counterpart to R2320 in C2 (Figure 3)] is the only residue observed to interact with the carboxylic acid group of the lipids, and only in a single trajectory. R2220 in FVIII C2 has no counterpart in FVIII C1; K2065 is the closest basic residue to this position according to structural alignment of the two domains, and this residue is positioned two residues downstream and interacts only nonspecifically with either of the negatively charged functional groups of the lipids (PO_4^- or COO^-).

Dynamical Interpretation of Hemophilic Missense Mutations and Antibody Epitopes Related to Membrane Binding. Our results offer a dynamical interpretation of the available hemophilia A disease genotypes related to dysfunctional membrane association and binding of FVIIIa via its dual discoidin domains (described in the previous section), a novel approach made possible by the use of the HMMM. Previous analyses have inferred the functional−structural causation of hemophilic missense mutations based upon either homology models[61,62] or X-ray crystallographic structures,[63] each of which offers only static representations of the protein structure in the absence of a membrane. Mutations of special interest are those positioned at the membrane-interacting surface of the C2-like domains and include the following basic residues: R2052, R2090, R2159, and R2163 in FVIII C1 and R2320 in FVIII C2. Caution must be taken when interpreting mutations. Potential pitfalls include not only the usual statistical fallacies but also unknown interactions with other biochemical components. With these precautions in mind, we here adopt the palatable concept that a hemophilic disease missense mutation located at the membrane-interacting surface patches of FVIII C1 or FVIII C2 is potentially due to improper membrane binding.

As has been noted previously,[63] it is remarkable that only few of the documented hemophilic missense mutations are positioned in the membrane-interacting patch (including the spikes) of the discoidin domains of FVIII (Figure 5). Specifically, only two mutants (V2223M, positioned between S2 and S3, and A2201P, located in S1) were proposed to disrupt membrane binding. This could suggest that the major components necessary for sufficient membrane interaction for FVIIIa *in vivo* are nonspecific contributions, such as hydrophobic partitioning and electrostatics, consistent with the results of the simulations described here. Furthermore, alanine scanning the FVIII C2 domain within a complete B-domain-less FVIII molecule has suggested that primarily residues in structural regions of the domain (β-sheet-forming residues) are functionally sensitive to mutation.[64] In addition to these general observations, our results further implicate R2163 in FVIII C1 and R2220 and R2320 in FVIII C2 as potentially critical residues in that they are the only basic residues capable of forming direct interactions with PS lipids. Notably, R2163 and R2320 are known to give rise to hemophilic conditions upon mutation [The Hemophilia A Mutation, Structure, Test and Resource Site (http://hadb.org.uk/)].

Antibodies KM33 and ESH-4 are known to modulate FVIII cellular uptake and binding.[18,19,65,66] KM33 abrogates the interaction between FVIII and phospholipids by binding to regions 2092 and 2093 within S3 of FVIII C1 and 2158 and 2159 within S4 of FVIII C1.[20] Analogously, ESH-4-binding epitopes have been narrowed down to regions 2192−2196 (N-terminal side of S1 of FVIII C2), 2210−2125 (containing S2 of FVIII C2), and 2313−2316 (S4 of FVIII C2).[67] A third FVIII antibody, ESH-8, which does not interfere with phospholipid binding, binds to residues 2234−2238 between S2 and S3 of FVIII C2 and to residues 2267−2270 between S3 and S4 of FVIII C2. Our results show excellent agreement with the binding epitopes of antibodies KM33, ESH-4, and ESH-8, in that the first two have epitopes located entirely within the membrane-contacting interface of C1 or C2, while the last one binds solely to regions not in contact with the membrane (Figure 5).

Proposed Mechanism of Membrane Interaction for Full-Length FVIII and Implications for a Putative FVIIIa:FIXa Tenase Complex. On the basis of our results for the membrane-bound states of FVIII C1 and FVIII C2, putative membrane-bound configurations of the intrinsic tenase complex are proposed. Overlaying the putative model of the FVIIIa:FIXa tenase complex (Figure 6A) with the converged

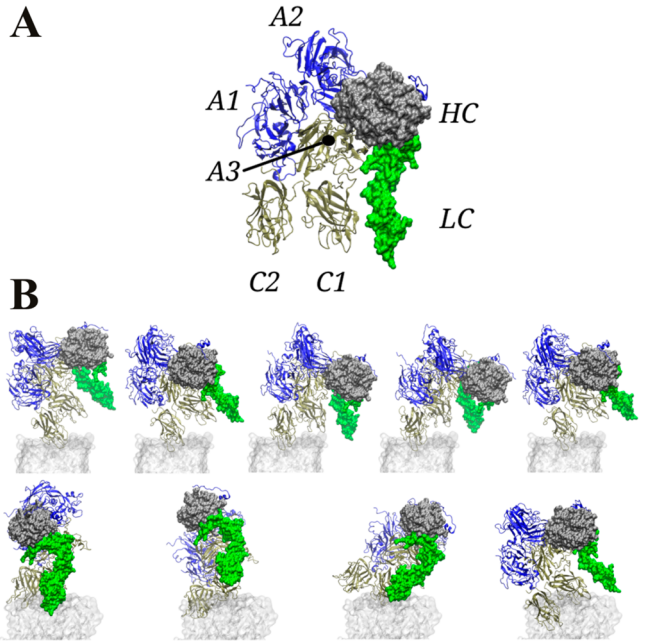

Figure 6. (A) Our constructed model of the FVIIIa:FIXa (tenase) complex. B-Domain deleted FVIIIa (domains A1−A2−A3−C1−C2) is shown in cartoon representation (A1−A2 colored blue, A3−C1−C2 colored tan). FIXa is drawn using a surface representation (HC, heavy chain colored gray; LC, light chain colored green). (B) Tenase complex model structurally aligned with and overlaid on the converged membrane-bound individual C2-like domains (top, C2/HMMM trajectories 1−5 from left to right, respectively; bottom, C1/HMMM trajectories 2−5 from left to right, respectively).

final membrane-bound orientations of the C2/HMMM simulations (Figure 6B, top), we find that, in all cases, preferential positioning of the C2 domain gives rise to tenase complex models without any clashes with the membrane. However, the N-terminally positioned Gla domain of FIXa at (around) its ω-loop is not in contact with the membrane, nor is the C1 domain of FVIII. There are structural models describing the interaction between membranes and the Gla domains from, e.g., prothrombin[68] and FVIIa,[69] which, due to the high degree of homology among Gla domains, is expected to be very similar to the mode of binding of the FIXa Gla domain to membranes. On the contrary, when FVIII is overlaid with the final FVIII C1 domain orientations from the C1/HMMM simulations (Figure

DOI: 10.1021/acs.biochem.5b00417
Biochemistry 2015, 54, 6123−6131

6B, bottom), two of the resulting orientations cause significant clashes between the FVIII C2 domain and the membrane (trajectories 3 and 5). Trajectories 2 and 4 of the C1/HMMM simulations correspond to reasonable modes of binding between the membrane and the tenase complex in which FVIII C1, FVIII C2, and FIXa Gla domains are all anchored in the membrane. Trajectory 2 looks intuitive where the entire complex is positioned normal to the membrane plane, while trajectory 4 is very similar to the highly tilted orientation suggested by FRET measurements.[24] To capture the motional span and membrane contact of the anchoring FVIII C1, FVIII C2, and FIX Gla of the putative tenase complex when they are overlaid with the performed membrane binding simulations, said tenase complex (Figure 6A) was structurally aligned to membrane-bound FVIII C2 (resulting from C2/HMMM simulations 1−5) or to membrane-bound FVIII C1 (for C1/HMMM simulations 2−5) in each simulation frame. The relative heights, z, of the FIX Gla ω-loop as well as spike 1 from the neighboring C domain reveal that realistic binding modes for the tenase complex are achieved only for the C1/HMMM simulations, primarily trajectory 2, but also transiently for trajectories 4 and 5 (Figure 7).

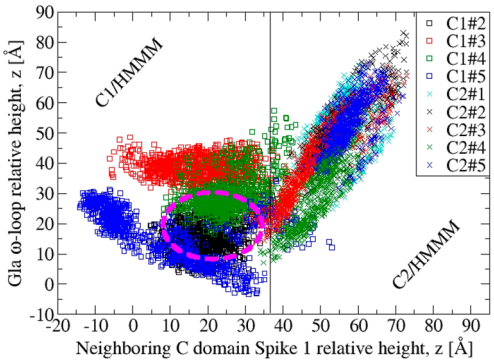

Figure 7. Scatter plot of relative heights, z, of the FIX Gla ω-loop (L6, α-carbon) as well as spike 1 from FVIII C2 (G2044, α-carbon) or FVIII C1 (M2199, α-carbon) calculated on the basis of structural alignment of the putative tenase complex model onto simulation trajectory frames from C2/HMMM (squares) or C1/HMMM (crosses). The abscissa shows the relative height of the neighboring C domain spike 1, i.e., FVIII C1 spike 1 for C2/HMMM trajectories, and vice versa. The ordinate shows in all cases the relative height of the FIX Gla domain ω-loop. The dashed ellipse (magenta) indicates relative heights corresponding to reasonable modes of interaction of the membrane-anchoring domains (roughly z = 15−25 Å). The vertical line approximately separates simulations C1/HMMM (mostly left) and C2/HMMM (mostly right). Individual trajectories are consistently color-coded (cyan for 1, black for 2, red for 3, green for 4, and blue for 5).

Collectively, these considerations indicate that optimal interaction between FVIII C2 and the membrane can be achieved without major domain rearrangements in FVIIIa, whereas FVIII C1 membrane interactions might induce domain rearrangements in FVIIIa. Bearing in mind the convergent nature of the FVIII C2 membrane interaction (described above) and the fact that the only nonbinding simulated system was C1/HMMM trajectory 1, we speculate that membrane association of FVIIIa is initiated by the FVIII C2 domain and that FVIII C1 facilitates further membrane anchoring while reorienting the cofactor. In any case, our simulations clearly indicate that FVIII C1 plays an important role in modulating the orientation of the FVIII molecule for optimal interaction with FIXa in the membrane-bound state. Because it is known that binding of FVIII to membranes involves a complex mechanism,[58] and considering the coiled nature of the four-residue FVIII C1−C2 interdomain linker (residues 2170−2173), domain rearrangements are plausible. The interdomain flexibility of full-length FVIIIa is unknown, in particular, whether and how the membrane selects for or induces certain relative domain configurations. Furthermore, there appear to be nontrivial differences in PS specificity for membrane binding of FVIII and FVIIIa.[70] However, preliminary results of simulations of the crystal structure of FVIII light chain bound to HMMM suggest that only minor relative domain rearrangements occur, supporting the validity of the presented rigid-body putative tenase complex model (data not shown). These concepts are intriguing and subjects for further studies.

CONCLUSION

Through the application of a novel membrane model with enhanced lipid dynamics, we have been able to describe spontaneous membrane binding and insertion of two membrane-anchoring domains of human coagulation FVIII. The simulations show that peripheral binding of FVIII C1 and FVIII C2 domains is facilitated by insertion of the domain-extruding spikes into the membrane. For FVIII C2, the resulting domain orientations converge to be nearly membrane-perpendicular, while FVIII C1 undergoes a structural change and is orientationally promiscuous (it can adopt several tilted orientations in the membrane-bound state). For both discoidin C2-like domains of FVIIIa, the mode of interaction with the phospholipid membrane is characterized by initial nonspecific attractive electrostatic interactions and hydrophobic partitioning. The insertion of the membrane-anchoring domain spikes is followed by the maturation of direct and specific interaction with a lipid molecule that enters the PS pocket. This specific lipid−protein interaction is observed more frequently and consistently for FVIII C2 than for FVIII C1. Deep embedding of large parts of either discoidin C2-like domain, as has been suggested for FVIII C2 on the basis of cryo-electron microscopy, is not observed.

ASSOCIATED CONTENT

Supporting Information

The Supporting Information is available free of charge on the ACS Publications website at DOI: 10.1021/acs.biochem.5b00417.

Supplemental Figures S1−S4 and atomic coordinates for the tenase complex model (PDF)

AUTHOR INFORMATION

Corresponding Authors

*Beckman Institute, 405 N. Mathews Ave., Urbana, IL 61801. Telephone: +1 217 244-6914. E-mail: emad@life.illinois.edu.

*Novo Nordisk A/S, Novo Nordisk Park, F5.1.29, DK-2760 Måløv, Denmark. Telephone: +45 3075 4511. E-mail: oho@novonordisk.com.

Present Address

⊥J.J.M.: Department of Chemistry, The University of Chicago, Chicago, IL 60637.

Author Contributions

J.J.M. designed the research, performed the research, analyzed data, and wrote the manuscript. Y.Z.O. designed the research,

DOI: 10.1021/acs.biochem.5b00417
Biochemistry 2015, 54, 6123−6131

contributed analytic tools, analyzed data, and revised the manuscript. G.H.P. and J.H.F. designed the research, analyzed data, and revised the manuscript. E.T. and O.H.O. designed the research, analyzed data, provided computational resources, and revised the manuscript.

Funding

This work is supported in part by Forsknings- og Innovationsstyrelsen (Danish Agency for Science, Technology and Innovation) and the Novo Nordisk R&D Science, Talent, Attraction and Recruitment (STAR) program (fellowship to J.J.M.) and the National Institutes of Health (Grants R01-GM101048, U54-GM087519, and P41-GM104601 to E.T.). All computation was performed on the Davinci supercomputer at Novo Nordisk and the TCBG linux PC clusters at UIUC.

Notes

The authors declare no competing financial interest.

REFERENCES

(1) MacFarlane, R. (1964) An enzyme cascade in the blood clotting mechanism, and its function as a biochemical amplifier. *Nature 202*, 498−499.

(2) Davie, E. W., and Ratnoff, O. D. (1964) Waterfall Sequence for Intrinsic Blood Clotting. *Science 145*, 1310−1312.

(3) Marder, V. J., Aird, W. C., Bennett, J. S., Schulman, S., and White, G. C. (2012) *Hemostasis and Thrombosis: Basic Principles and Clinical Practice*, 6th ed., Lippincott Williams & Wilkins, Philadelphia.

(4) Van Dieijen, G., Tans, G., Rosing, J., and Hemker, H. C. (1981) The Role of Phospholipid and Factor VIIIa in the Activation of Bovine Factor X. *J. Biol. Chem. 256*, 3433−3442.

(5) Lemmon, M. A. (2008) Membrane recognition by phospholipid-binding domains. *Nat. Rev. Mol. Cell Biol. 9*, 99−111.

(6) Wakabayashi, H., Griffiths, A. E., and Fay, P. J. (2010) Factor VIII lacking the C2 domain retains cofactor activity in vitro. *J. Biol. Chem. 285*, 25176−25184.

(7) Pratt, K. P., Shen, B. W., Takeshima, K., Davie, E. W., Fujikawa, K., and Stoddard, B. L. (1999) Structure of the C2 domain of human factor VIII at 1.5Å resolution. *Nature 402*, 439−442.

(8) Hsu, T.-C., Pratt, K. P., and Thompson, A. R. (2008) The factor VIII C1 domain contributes to platelet binding. *Blood 111*, 200−208.

(9) Pantazatos, D., Gessner, C. R., Woods, V. L., Jr., and Gilbert, G. E. (2014) Changes in the Factor VIII C2 Domain upon Membrane Binding Determined by Deuterium Exchange Mass Spectroscopy. *Biochem. J. 461*, 443−451.

(10) Gilbert, G. E. (2013) Factor VIII inhibitor epitopes and an enigma. *Blood 122*, 4160−4161.

(11) Sharon, N., and Lis, H. (2003) *Lectins*, 2nd ed., Springer, Berlin.

(12) Mertens, K., and Meijer, A. B. (2012) Factors VIII and V swap fatty feet. *Blood 120*, 1761−1763.

(13) Macedo-Ribeiro, S., Bode, W., Huber, R., Quinn-Allen, M. A., Kim, S. W., Ortel, T. L., Bourenkov, G. P., Bartunik, H. D., Stubbs, M. T., Kane, W. H., and Fuentes-Prior, P. (1999) Crystal structures of the membrane-binding C2 domain of human coagulation factor V. *Nature 402*, 434−439.

(14) Gilbert, G. E., Kaufman, R. J., Arena, A. A., Miao, H., and Pipe, S. W. (2002) Four hydrophobic amino acids of the factor VIII C2 domain are constituents of both the membrane-binding and von Willebrand factor-binding motifs. *J. Biol. Chem. 277*, 6374−6381.

(15) Gilbert, G. E., Novakovic, V. A., Kaufman, R. J., Miao, H., and Pipe, S. W. (2012) Conservative mutations in the C2 domains of factor VIII and factor V alter phospholipid binding and cofactor activity. *Blood 120*, 1923−1932.

(16) Foster, P. A., Fulcher, C. A., Houghten, R. A., and Zimmerman, T. S. (1990) Synthetic factor VIII peptides with amino acid sequences contained within the C2 domain of factor VIII inhibit factor VIII binding to phosphatidylserine. *Blood 75*, 1999−2004.

(17) Lü, J., Pipe, S. W., Miao, H., Jacquemin, M., and Gilbert, G. E. (2011) A membrane-interactive surface on the factor VIII C1 domain cooperates with the C2 domain for cofactor function. *Blood 117*, 3181−3189.

(18) Meems, H., Meijer, A. B., Cullinan, D. B., Mertens, K., and Gilbert, G. E. (2009) Factor VIII C1 domain residues Lys 2092 and Phe 2093 contribute to membrane binding and cofactor activity. *Blood 114*, 3938−3946.

(19) Meems, H., van den Biggelaar, M., Rondaij, M., van der Zwaan, C., Mertens, K., and Meijer, A. B. (2011) C1 domain residues Lys 2092 and Phe 2093 are of major importance for the endocytic uptake of coagulation factor VIII. *Int. J. Biochem. Cell Biol. 43*, 1114−1121.

(20) Bloem, E., van den Biggelaar, M., Wroblewska, A., Voorberg, J., Faber, J. H., Kjalke, M., Stennicke, H. R., Mertens, K., and Meijer, A. B. (2013) Factor VIII C1 Domain Spikes 2092−2093 and 2158−2159 Comprise Regions That Modulate Cofactor Function and Cellular Uptake. *J. Biol. Chem. 288*, 29670−29679.

(21) Wakabayashi, H., and Fay, P. J. (2013) Replacing the factor VIII C1 domain with a second C2 domain reduces factor VIII stability and affinity for factor IXa. *J. Biol. Chem. 288*, 31289−31297.

(22) Ngo, J. C. K., Huang, M., Roth, D. A., Furie, B. C., and Furie, B. (2008) Crystal structure of human factor VIII: implications for the formation of the factor IXa-factor VIIIa complex. *Structure 16*, 597−606.

(23) Liu, Z., Lin, L., Yuan, C., Nicolaes, G. A. F., Chen, L., Meehan, E. J., Furie, B., Furie, B., and Huang, M. (2010) Trp2313-His2315 of factor VIII C2 domain is involved in membrane binding: structure of a complex between the C2 domain and an inhibitor of membrane binding. *J. Biol. Chem. 285*, 8824−8829.

(24) Wakabayashi, H., and Fay, P. J. (2013) Molecular orientation of Factor VIIIa on the phospholipid membrane surface determined by fluorescence resonance energy transfer. *Biochem. J. 452*, 293−301.

(25) Parmenter, C. D. J., Cane, M. C., Zhang, R., and Stoilova-McPhie, S. (2008) Cryo-electron microscopy of coagulation Factor VIII bound to lipid nanotubes. *Biochem. Biophys. Res. Commun. 366*, 288−293.

(26) Stoilova-McPhie, S., Parmenter, C. D. J., Segers, K., Villoutreix, B. O., and Nicolaes, G. A. F. (2008) Defining the structure of membrane-bound human blood coagulation factor Va. *J. Thromb. Haemostasis 6*, 76−82.

(27) Stoilova-McPhie, S., Lynch, G. C., Ludtke, S., and Pettitt, B. M. (2013) Domain organization of membrane-bound factor VIII. *Biopolymers 99*, 448−459.

(28) Miller, J., Dalm, D., Koyfman, A. Y., Grushin, K., and Stoilova-McPhie, S. (2014) Helical organization of blood coagulation factor VIII on lipid nanotubes. *J. Visualized Exp. 88*, e51254.

(29) Chaves, R. C., Dahmane, S., Odorico, M., Nicolaes, G. A. F., and Pellequer, J. L. (2014) Factor Va alternative conformation reconstruction using atomic force microscopy. *Thromb. Haemostasis 112*, 1167−1173.

(30) Du, J., Wichapong, K., Hackeng, T. M., and Nicolaes, G. A. F. (2015) Molecular simulation studies of human coagulation factor VIII C domain-mediated membrane binding. *Thromb. Haemostasis 113*, 373−384.

(31) Ohkubo, Y. Z., Pogorelov, T. V., Arcario, M. J., Christensen, G. A., and Tajkhorshid, E. (2012) Accelerating membrane insertion of peripheral proteins with a novel membrane mimetic model. *Biophys. J. 102*, 2130−2139.

(32) Pogorelov, T. V., Vermaas, J. V., Arcario, M. J., and Tajkhorshid, E. (2014) Partitioning of amino acids into a model membrane: Capturing the interface. *J. Phys. Chem. B 118*, 1481−1492.

(33) Li, H., Robertson, A. D., and Jensen, J. H. (2005) Very fast empirical prediction and rationalization of protein pKa values. *Proteins: Struct., Funct., Genet. 61*, 704−721.

(34) Martínez, L., Andrade, R., Birgin, E. G., and Martínez, J. M. (2009) Packmol: A Package for Building Initial Configurations. *J. Comput. Chem. 30*, 2157−2164.

(35) Humphrey, W., Dalke, A., and Schulten, K. (1996) VMD: visual molecular dynamics. *J. Mol. Graphics 14*, 33−38.

(36) Nagle, J. F., and Tristram-Nagle, S. (2000) Structure of lipid bilayers. *Biochim. Biophys. Acta, Rev. Biomembr. 1469*, 159−195.

DOI: 10.1021/acs.biochem.5b00417
Biochemistry 2015, 54, 6123−6131

(37) Petrache, H. I., Tristram-Nagle, S., Gawrisch, K., Harries, D., Parsegian, V. A., and Nagle, J. F. (2004) Structure and fluctuations of charged phosphatidylserine bilayers in the absence of salt. *Biophys. J. 86*, 1574−1586.
(38) Martyna, G. J., Tobias, D. J., and Klein, M. L. (1994) Constant pressure molecular dynamics algorithms. *J. Chem. Phys. 101*, 4177−4189.
(39) Feller, S. E., Zhang, Y. H., Pastor, R. W., and Brooks, B. R. (1995) Constant pressure molecular dynamics simulation: The Langevin piston method. *J. Chem. Phys. 103*, 4613−4621.
(40) Allen, M. P., and Tildesley, D. J. (1989) *Computer simulation of liquids*, Reprint Edition, Oxford University Press, Oxford, U.K.
(41) Darden, T., York, D., and Pedersen, L. (1993) Particle mesh Ewald: An $N\bullet\log(N)$ method for Ewald sums in large systems. *J. Chem. Phys. 98*, 10089−10092.
(42) Essmann, U., Perera, L., Berkowitz, M. L., Darden, T., Lee, H., and Pedersen, L. G. (1995) A smooth particle mesh Ewald method. *J. Chem. Phys. 103*, 8577−8592.
(43) Phillips, J. C., Braun, R., Wang, W., Gumbart, J., Tajkhorshid, E., Villa, E., Chipot, C., Skeel, R. D., Kalé, L., and Schulten, K. (2005) Scalable molecular dynamics with NAMD. *J. Comput. Chem. 26*, 1781−1802.
(44) MacKerell, A. D., Bashford, D., Bellott, M., Dunbrack, R. L., Evanseck, J. D., Field, M. J., Fischer, S., Gao, J., Ha, S., Joseph-McCarthy, D., Kuchnir, L., Kuczera, K., Lau, F. T. K., Mattos, C., Michnick, S., Ngo, T., Nguyen, D. T., Prodhom, B., Reiher, W. E., Roux, B., Schlenkrich, M., Smith, J. C., Stote, R., Straub, J., Watanabe, M., Wiórkiewich-Kuczera, J., Yin, D., and Karplus, M. (1998) All-atom empirical potential for molecular modeling and dynamics studies of proteins. *J. Phys. Chem. B 102*, 3586−3616.
(45) MacKerell, A. D., Feig, M., and Brooks, C. L. (2004) Extending the treatment of backbone energetics in protein force fields: limitations of gas-phase quantum mechanics in reproducing protein conformational distributions in molecular dynamics simulations. *J. Comput. Chem. 25*, 1400−1415.
(46) Best, R. B., Zhu, X., Shim, J., Lopes, P. E. M., Mittal, J., Feig, M., and MacKerell, A. D. (2012) Optimization of the additive CHARMM all-atom protein force field targeting improved sampling of the backbone φ, ψ and side-chain $\chi(1)$ and $\chi(2)$ dihedral angles. *J. Chem. Theory Comput. 8*, 3257−3273.
(47) Jorgensen, W. L., Chandrasekhar, J., Madura, J. D., Impey, R. W., and Klein, M. L. (1983) Comparison of simple potential functions for simulating liquid water. *J. Chem. Phys. 79*, 926−935.
(48) Ryckaert, J., Ciccotti, G., and Berendsen, H. (1977) Numerical integration of the cartesian equations of motion of a system with constraints: molecular dynamics of n-alkanes. *J. Comput. Phys. 23*, 327−341.
(49) Cecchini, M., Rao, F., Seeber, M., and Caflisch, A. (2004) Replica exchange molecular dynamics simulations of amyloid peptide aggregation. *J. Chem. Phys. 121*, 10748−10756.
(50) Lechtenberg, B. C., Murray-Rust, T. A., Johnson, D. J., Adams, T. E., Krishnaswamy, S., Camire, R. M., and Huntington, J. A. (2013) Crystal structure of the prothrombinase complex from the venom of Pseudonaja textilis. *Blood 122*, 2777−2783.
(51) Banner, D. W., D'Arcy, A., Chène, C., Winkler, F. K., Guha, A., Konigsberg, W. H., Nemerson, Y., and Kirchhofer, D. (1996) The crystal structure of the complex of blood coagulation factor VIIa with soluble tissue factor. *Nature 380*, 41−46.
(52) Brandstetter, H., Bauer, M., Huber, R., Lollar, P., and Bode, W. (1995) X-ray structure of clotting factor IXa: active site and module structure related to Xase activity and hemophilia B. *Proc. Natl. Acad. Sci. U. S. A. 92*, 9796−9800.
(53) Novakovic, V. A., Cullinan, D. B., Wakabayashi, H., Fay, P. J., Baleja, J. D., and Gilbert, G. E. (2011) Membrane-binding properties of the Factor VIII C2 domain. *Biochem. J. 435*, 187−196.
(54) Lomize, M. A., Lomize, A. L., Pogozheva, I. D., and Mosberg, H. I. (2006) OPM: orientations of proteins in membranes database. *Bioinformatics 22*, 623−625.
(55) Shen, B. W., Spiegel, P. C., Chang, C.-H., Huh, J.-W., Lee, J.-S., Kim, J., Kim, Y.-H., and Stoddard, B. L. (2007) The tertiary structure and domain organization of coagulation factor VIII. *Blood 111*, 1240−1247.
(56) Ohkubo, Y. Z., and Tajkhorshid, E. (2013) Exploring Membrane-Bound form of the C2 Domain by HMMM Model. *Biophys. J. 104*, 432a.
(57) Mulgrew-Nesbitt, A., Diraviyam, K., Wang, J., Singh, S., Murray, P., Li, Z., Rogers, L., Mirkovic, N., and Murray, D. (2006) The role of electrostatics in protein-membrane interactions. *Biochim. Biophys. Acta, Mol. Cell Biol. Lipids 1761*, 812−826.
(58) Bardelle, C., Furie, B., Furie, B. C., and Gilbert, G. E. (1993) Membrane binding kinetics of factor VIII indicate a complex binding process. *J. Biol. Chem. 268*, 8815−8824.
(59) Bernstein, F. C., Koetzle, T. F., Williams, G. J. B., Meyer, E. F., Brice, M. D., Rodgers, J. R., Kennard, O., Shimanouchi, T., and Tasumi, M. (1977) The Protein Data Bank: a computer-based archival file for macromolecular structures. *J. Mol. Biol. 112*, 535−542.
(60) Svensson, L. A., Thim, L., Olsen, O. H., and Nicolaisen, E. M. (2013) Evaluation of the metal binding sites in a recombinant coagulation factor VIII identifies two sites with unique metal binding properties. *Biol. Chem. 394*, 761−765.
(61) Pellequer, J. L., Gale, A. J., Griffin, J. H., and Getzoff, E. D. (1998) Homology models of the C domains of blood coagulation factors V and VIII: a proposed membrane binding mode for FV and FVIII C2 domains. *Blood Cells, Mol., Dis. 24*, 448−461.
(62) Gale, A. J., Pellequer, J. L., Getzoff, E. D., and Griffin, J. H. (2000) Structural basis for hemophilia A caused by mutations in the C domains of blood coagulation factor VIII. *Thromb. Haemost. 83*, 78−85.
(63) Liu, M. L., Shen, B. W., Nakaya, S., Pratt, K. P., Fujikawa, K., Davie, E. W., Stoddard, B. L., and Thompson, A. R. (2000) Hemophilic factor VIII C1- and C2-domain missense mutations and their modeling to the 1.5-angstrom human C2-domain crystal structure. *Blood 96*, 979−987.
(64) Pellequer, J. L., Chen, S. W., Saboulard, D., Delcourt, M., Négrier, C., and Plantier, J. L. (2011) Functional mapping of factor VIII C2 domain. *Thromb. Haemostasis 106*, 121−131.
(65) Wroblewska, A., van Haren, S. D., Herczenik, E., Kaijen, P., Ruminska, A., Jin, S.-Y., Zheng, X. L., van den Biggelaar, M., ten Brinke, A., Meijer, A. B., and Voorberg, J. (2012) Modification of an exposed loop in the C1 domain reduces immune responses to factor VIII in hemophilia A mice. *Blood 119*, 5294−5300.
(66) Brinkman, H.-J. M., Mertens, K., and van Mourik, J. A. (2002) Phospholipid-Binding Domain of Factor VIII Is Involved in Endothelial Cell-Mediated Activation of Factor X by Factor IXa. *Arterioscler., Thromb., Vasc. Biol. 22*, 511−516.
(67) Faber, J. H., Appa, R. S., Stennicke, H., and Kjalke, M. (2013) Contribution of C2 domain epitopes in FVIII cellular uptake assessed by epitope mapping of the anti-C2 antibodies ESH4 and ESH8 by hydrogen-deuterium exchange mass spectrometry. FASEB Summer Research Conference on Proteases in Hemostasis & Vascular Biology, June 2−7, Nassau, Bahamas.
(68) Huang, M., Rigby, A. C., Morelli, X., Grant, M. A., Huang, G., Furie, B., Seaton, B., and Furie, B. C. (2003) Structural basis of membrane binding by Gla domains of vitamin K-dependent proteins. *Nat. Struct. Biol. 10*, 751−756.
(69) Ohkubo, Y. Z., and Tajkhorshid, E. (2008) Distinct structural and adhesive roles of Ca^{2+} in membrane binding of blood coagulation factors. *Structure 16*, 72−81.
(70) Engelke, H., Lippok, S., Dorn, I., Netz, R. R., and Rädler, J. O. (2011) FVIII binding to PS membranes differs in the activated and non-activated form and can be shielded by annexin A5. *J. Phys. Chem. B 115*, 12963−12970.

DOI: 10.1021/acs.biochem.5b00417
Biochemistry 2015, 54, 6123−6131